The Whi2p-Psr1p/Psr2p complex regulates interference competition and expansion of cells with competitive advantage in yeast colonies

Jana Maršíková[a,1], Martina Pavlíčková[b,1], Derek Wilkinson[a], Libuše Váchová[b], Otakar Hlaváček[b], Ladislava Hatáková[a], and Zdena Palková[a,2]

[a]Department of Genetics and Microbiology, Faculty of Science, Charles University, BIOCEV, 128 00 Prague, Czech Republic; and [b]Institute of Microbiology of the Czech Academy of Sciences, BIOCEV, 142 20 Prague, Czech Republic

Edited by E. Peter Greenberg, University of Washington, Seattle, WA, and approved May 13, 2020 (received for review December 20, 2019)

Yeast form complex highly organized colonies in which cells undergo spatiotemporal phenotypic differentiation in response to local gradients of nutrients, metabolites, and specific signaling molecules. Colony fitness depends on cell interactions, cooperation, and the division of labor between differentiated cell subpopulations. Here, we describe the regulation and dynamics of the expansion of papillae that arise during colony aging, which consist of cells that overcome colony regulatory rules and disrupt the synchronized colony structure. We show that papillae specifically expand within the U cell subpopulation in differentiated colonies. Papillae emerge more frequently in some strains than in others. Genomic analyses further revealed that the Whi2p-Psr1p/Psr2p complex (WPPC) plays a key role in papillae expansion. We show that cells lacking a functional WPPC have a sizable interaction-specific fitness advantage attributable to production of and resistance to a diffusible compound that inhibits growth of other cells. Competitive superiority and high relative fitness of *whi2* and *psr1psr2* strains are particularly pronounced in dense spatially structured colonies and are independent of TORC1 and Msn2p/Msn4p regulators previously associated with the WPPC function. The WPPC function, described here, might be a regulatory mechanism that balances cell competition and cooperation in dense yeast populations and, thus, contributes to cell synchronization, pattern formation, and the expansion of cells with a competitive fitness advantage.

yeast multicellularity | interference competition | interaction-specific fitness inequality | chimeric populations | competitive advantage

In most natural settings, microbes exist in structured communities where cells interact, communicate, and differentiate into specific forms. Positive or negative social interactions, such as cooperation or competition among microbes, affect communities' structural complexity (1). Cellular interactions can also affect the survival and reproductive potential of the whole population as well as its constituents. Positive interactions among different microbes result in complex multispecies biofilms that protect their constituents from environmental insults, including antimicrobial drugs (2). Knowledge of interactions in evolving microbial communities is, therefore, essential for understanding how microbes influence everyday human life, whether as biofilms formed by pathogens, as beneficial gut flora, or as microbial consortia used to produce food or to remediate environmental contaminants (3–5).

Depending on their complexity, microbial populations can display multicellular attributes, including cell differentiation and cooperation, division of labor and the secretion of public goods (e.g., metabolites, enzymes, toxins, and signaling molecules). Cooperative behavior is vulnerable to exploitation by cheater mutants that exploit the population by using but not producing public goods (6). Cheaters´ fitness advantage can negatively impact the population from which they arise, such as by compromising the biofilm structure, fitness, and stress resistance (7). However, the presence of cheaters also increases the genetic diversity of the population and, thus, its adaptive potential. One form of cheating is "interaction-specific fitness inequality" in which one cell line behaves like another in a pure (unmixed) culture but exploits the other cell line in a chimeric (mixed) culture (8, 9) (see the *SI Appendix* for related definitions and other terms). Interaction-dependent cell competition can take the form of interference competition, such as when a compound produced by one strain harms another strain during their interaction (a form of allelopathy) (10, 11).

Another important feature of multicellular communities is their spatial structure, controlled by various factors that drive cell spatial organization and differentiation. During group formation, cells can come together and, subsequently, specialize, e.g., myxobacteria and multispecies bacterial biofilms (12, 13); alternatively, cells can stay together after cell division. Multicellular clusters of *Saccharomyces cerevisiae* (snowflake yeast) that arise during experimental evolution (14, 15) exemplify the latter strategy and illustrate how the secretion and use of public goods

Significance

Population structure and spatiotemporal dynamics in natural microbial communities largely depend on interactions of constituent cells with each other and the environment. Using a yeast colony model, we identified the Whi2p-Psr1p/Psr2p complex as an important interference competition regulator that strongly influences cell interactions, pattern formation, and adaptive potential in dense yeast populations. In the presence of this complex, the offspring of potentially fitter mutants that emerged in developing colonies rapidly grow and outcompete parental cells by forming papillae specifically localized within the colony. Papillae expansion disrupts colony organization in a manner that resembles tissue disruption by tumor cells. Cells with a dysfunctional complex acquire interaction-specific fitness dominance and rapidly exclude cells with a functional complex from the population.

Author contributions: L.V. and Z.P. designed research; J.M., M.P., L.V., O.H., L.H., and Z.P. performed research; J.M., M.P., D.W., L.V., O.H., and Z.P. analyzed data; and D.W., L.V., and Z.P. wrote the paper.

The authors declare no competing interest.

This article is a PNAS Direct Submission.

Data deposition: The sequencing data were deposited in the National Center for Biotechnology Information's (NCBI) Sequence Read Archive (accession no. PRJNA542361). The proteomics data were deposited to the ProteomeXchange Consortium via the Proteomics Identifications Database (PRIDE) (accession no. PXD016670).

[1]J.M. and M.P. contributed equally to this work.

[2]To whom correspondence may be addressed. Email: zdenap@natur.cuni.cz.

This article contains supporting information online at https://www.pnas.org/lookup/suppl/doi:10.1073/pnas.1922076117/-/DCSupplemental.

First published June 15, 2020.

can lead to selection for incomplete cell separation (16). Complex colony structures formed by the division of nonmotile yeast cells (17) also typify staying together, although passive cell movement driven by physical forces can occur within these structures.

The study of colony formation and differentiation in a tractable model organism, such as baker's yeast, facilitates identification of molecular mechanisms underlying cell–cell interactions. Colonies may consist of populations arising either from a single cell (microcolonies) or from a collection of genetically identical cell ancestors (giant colonies formed from a drop of cell suspension) (18, 19). Colonies exhibit precise spatiotemporal organization, controlled by the integration of genetic programming and environmental signals (17) in the form of nutrient gradients and gradients of various metabolites and signaling molecules. Because cell differentiation is influenced by the local environment, spatial patterns arise as colonies age in which certain cell types become localized to specific regions (17, 20). Phenotypic differentiation can result in U cell variants in upper regions and L cell variants in lower regions (19, 21). Like soma in a multicellular organism, U cells and L cells are genetically identical but physiologically distinct. Differentiation begins at the very top and bottom of the colony, and as differentiation proceeds, the boundary between the U and the L cells becomes progressively sharper (Fig. 1*A*) (21). Extracellular ammonia, a quorum-sensing molecule produced by U cells, is the only signal that has so far been confirmed to participate in U/L cell differentiation and colony synchronization (17–19, 21). Defects in ammonia signaling and U/L cell differentiation decrease the long-term viability of a colony (21, 22).

In fully differentiated colonies, U cells activate a unique adaptive metabolism and become long lived relative to L cells. Interestingly, U cells behave like quiescent stress-resistant cells in certain respects and like metabolically active slowly dividing cells in others. In contrast, starving L cells remain in a resting state and activate various hydrolytic pathways (21). Evidence for division of labor exists between U and L cells. L cells release nutritive compounds (public goods) that are consumed predominantly by U cells (21, 23) since L cells, likely due to their metabolic state, do not consume these compounds themselves. As a result, the fitness of U cells (which retain the reproductive potential) is enhanced, whereas that of L cells is reduced. When specific mutations prevent the development of typical L cells, the viability of U cells and of the whole colony is negatively affected (21). The sharing of specific metabolic properties by U cells and others by L cells suggests communication and cooperation among cells within each of the two colony layers. Thus, the development of individual U cells is not independent but rather synchronized in terms of metabolism and other features (17, 21). Coordinated slow growth (21) likely enables U cells to economically utilize available nutrients (common resources), which become limited in older colonies. However, among coordinated cells, faster-growing individuals can appear, disrupting the structure and forming papillae—small protuberances on the colony surface—which are also formed by mutated cells in bacterial colonies (24).

Loss-of-function (LOF) mutations in the *WHI2* gene often appear as secondary mutations in a yeast deletion collection and in evolutionary screens (25–29). A major role in the general stress response has been attributed to Whi2p together with its interacting partners protein phosphatases Psr1p/Psr2p and transcription factor Msn2p (30). Whi2p has been implicated in other processes, including the degradation of misfolded proteins (25), mitophagy (31), cell death (32), resistance to some stresses (32–34), and the regulation of TORC1 (35, 36). *WHI2* shares structural similarity with the mammalian KCTD family proteins (28), members of which have been implicated in various diseases (37), although their functions remain poorly understood.

Here, we show that cells with fitness advantages develop in yeast colonies and specifically overgrow the U cell subpopulation to form papillae. Papillae propagation requires a functional Whi2p-Psr1p/Psr2p complex (WPPC). Complex dysfunctionality yields cells with a competitive superiority, which outcompete any cells with a functional complex via interference competition by production of an extracellular inhibiting compound. This prevents expansion of cells with other potentially beneficial mutations, reducing the adaptive potential of the population.

Results

WPPC Regulates the Propagation of Lineages of Fitter Cells among U Cells Independently of Msn2p/Msn4p and TORC1. The plating of *S. cerevisiae* strain BY4742 on glycerol medium agar (GMA) yielded two distinct types of microcolonies that differ in the number of papillae forming on their surface. Papillae were formed by cells that grew faster than other colony cells and disrupted the colony structure. These cells (hereafter called "papillae cells" [PCs]) harbor beneficial mutations or epigenetic changes. Microcolonies and giant colonies with few PCs had smooth morphologies (smooth colonies), whereas colonies with many such cells formed numerous papillae and sectors (papillating colonies) (Figs. 1*B* and 2*A* and *SI Appendix*, Fig. S1 and Table S1). As microcolonies are derived from single cells,

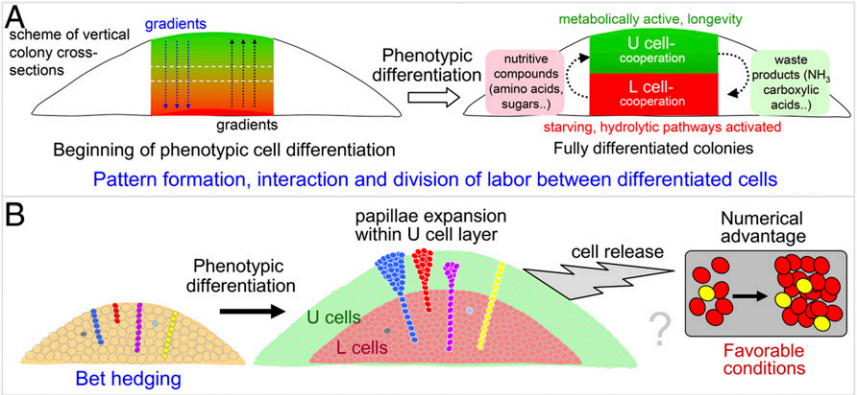

Fig. 1. Scheme of colony differentiation, bet hedging, and papillae expansion. (*A*) Phenotypic differentiation of *S. cerevisiae* colonies shown in schematic vertical cross sections of young and fully differentiated colonies. (*B*) Low-frequency cell types arise by mutations or heritable epigenetic changes in developing colonies, increasing cell heterogeneity. Some of these cells gain a fitness advantage and grow faster within the U cell layer, resulting in a numerical advantage after cells are dispersed from colonies, which could form the basis of subsequent competitive success (e.g., red papillae and yellow nonpapillae cell comparison, shown).

papillae evolve de novo during colony development. The smooth and papillating phenotypes were stable after replating with smooth colonies appearing only occasionally among papillating colonies. Papillae gradually appeared in papillating giant colonies, becoming visible to the naked eye after ∼10 d of colony growth (Fig. 2*A*). Microscopy of colony vertical cross sections revealed that PCs propagated as funnel-shaped structures mostly in the U cell subpopulation (Fig. 2 *C* and *D*). Approximately 200 papillae on average were detected on the surface of 18-d-old giant papillating colonies (Fig. 2*B*), and PCs occupied ∼24% of the U cell area (*SI Appendix*, Fig. S2).

Whole-genome resequencing of three randomly selected clones (S1–S3) forming smooth colonies and three clones (P1–P3) forming papillating colonies revealed mutations in individual clones. A single-nucleotide polymorphism in the *WHI2* gene ($whi2_{C598T}$) leading to the gain of a stop codon and thereby a 287-residue C-terminal truncation ($Whi2p^{Gln200X}$) was common to all three S clones but did not appear in the three P clones (*SI Appendix*, Table S2 and Fig. S3). Comparison of colonies of P1 and a P1-derived *whi2*Δ strain (P1-*whi2*) suggested that full-length Whi2p is responsible for the formation of papillating colonies (Fig. 2*A*). Deletion of the $whi2_{C598T}$ allele had no apparent effect on colony morphology or papillae frequency since this strain behaved similarly to S1 and P1-*whi2*.

Whi2p together with Psr1p/Psr2p activate the stress-response regulator Msn2p (30). We, therefore, examined the roles of Psr1p and Msn2p and their paralogs Psr2p and Msn4p in papillae emergence. P1-*psr1psr2* colonies behaved similarly to P1-*whi2* colonies and exhibited a smooth phenotype, whereas the single deletion of *PSR1* or *PSR2* only partially reduced papillae appearance. The deletion of *MSN2* and/or *MSN4* had no effect on papillae formation (Fig. 2*B*). The presence or absence of functional Whi2p alone did not seem to affect colony differentiation since both papillating (P1) and smooth ($whi2_{C598T}$ or P1-*whi2*) colonies (Fig. 2 *C* and *D*) exhibited typical U and L cells (19, 21) and TORC1 activity. TORC1 was inactive prior to cell differentiation and in L cells but active in U cells in both papillating and smooth colonies (*SI Appendix*, Fig. S4).

Whi2p Does Not Affect the Mutation Rate in Colonies. The sequencing of the three P and three S clones identified a comparable number of genomic mutations in both groups. We then estimated the mutation rate using a standard test (38), which involves measuring random LOF mutations in the gene for the arginine transporter Can1p. Can1p imports canavanine (a toxic arginine analog); thus, LOF mutations in *CAN1* impart canavanine resistance (CanR). The numbers of CanR clones in both overnight cell cultures and cells separated from the upper and lower regions of colonies of strains P1, P1-*whi2*, and P1-p_{TEF}-*WHI2*, which constitutively express Whi2p, were quantified. A similar CanR frequency (between 10^{-6} and 5×10^{-6}) was found for all strains and setups (*SI Appendix*, Fig. S5), which indicated that Whi2p did not affect mutation rates under the tested conditions.

The Absence of Whi2p or Psr1p/Psr2p Leads to Increased Fitness in Chimeric Colonies. We mixed a P1 strain constitutively expressing green fluorescent protein (GFP) (P1-p_{TEF}-GFP) at a 1:1 ratio with P1 strains deleted for *WHI2*, *PSR1*, *PSR2*, or both *PSR1* and *PSR2* (*SI Appendix*, Table S1). We then investigated chimerism in mixed colonies by microscopy (Fig. 3*A*) and determined the frequencies of fluorescent and nonfluorescent cell types (Fig. 3*B*). Although no selective advantage was observed between P1 and P1-p_{TEF}-GFP cells, competitive exclusion of P1-p_{TEF}-GFP by P1-*whi2* cells was visible in 4-d-old mixed colonies and became increasingly apparent at the later stages of colony growth. Similar competitive exclusion was observed between P1-*psr1psr2* and P1-p_{TEF}-GFP cells. The relative fitness of P1-*whi2* and P1-*psr1psr2* after 15 d (nine generations, on average) was 1.4–1.5 (Fig. 3*G*), demonstrating a strong fitness advantage of these strains over P1-p_{TEF}-GFP in colonies. We detected no difference in the growth of single-strain colonies of P1, P1-*whi2*, and P1-*psr1psr2* on GMA over ∼25 d (Fig. 3*C*), suggesting that the competitive advantage was not simply due to the rapid growth of the P1-*whi2* (P1-*psr1psr2*) strain but rather to interaction-dependent fitness inequalities in mixed colonies. P1-*psr1* and P1-*psr2* cells exhibited relatively smaller but significant competitive advantages over P1-p_{TEF}-GFP cells, implying divergent functions and/or abundance differences in the two proteins. Their frequencies in mixed colonies increased less rapidly (Fig. 3*B*), and the relative fitness of P1-*psr1* and P1-*psr2* at 15 d (compared with that of P1-p_{TEF}-GFP) was lower than that of P1-*whi2* and P1-*psr1psr2* (Fig. 3*G*).

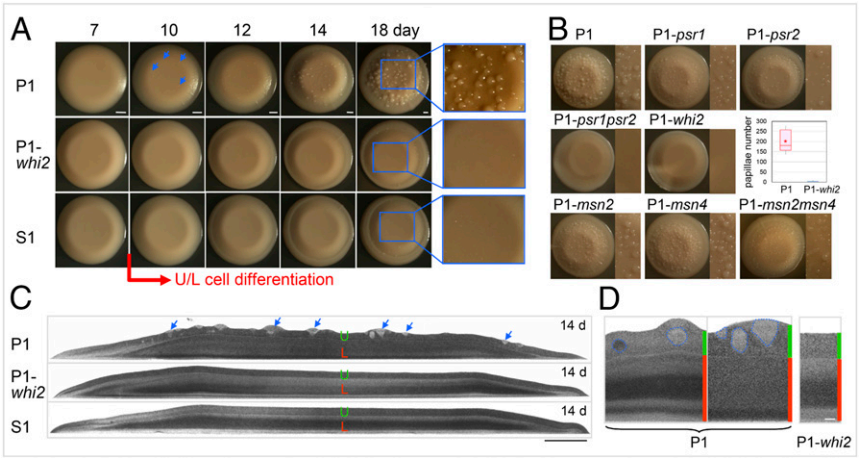

Fig. 2. Papillae in P1 and mutated colonies. (*A*) Formation of papillae in the colonies of P1, P1-*whi2*, and S1 strains. The *Inset* (18-d-old colonies) shows the colony surface at a higher magnification. (Scale bars, 1 mm.). (*B*) Papillae in 18-d-old colonies of P1 and knockout (KO) strains. The box plot shows the distribution of the number of visible papillae on the surface of P1 and P1-*whi2* colonies. (*C*) Cross sections of 14-d-old colonies as in *A*, visualized by transmitted light. U and L cells are indicated. Subpopulations of PCs within U cells of the P1 strain (examples indicated with arrows). (Scale bar, 1 mm.) (*D*) *Insets* of the cross sections of P1 and P1-*whi2* colonies showing different locations of papillae. PC regions surrounded by a blue dotted line. The positions of U and L cells are indicated with green and red bars, respectively. In P1 colonies, the regular U cell layer is partially disrupted by PCs. (Scale bar, 100 μm.)

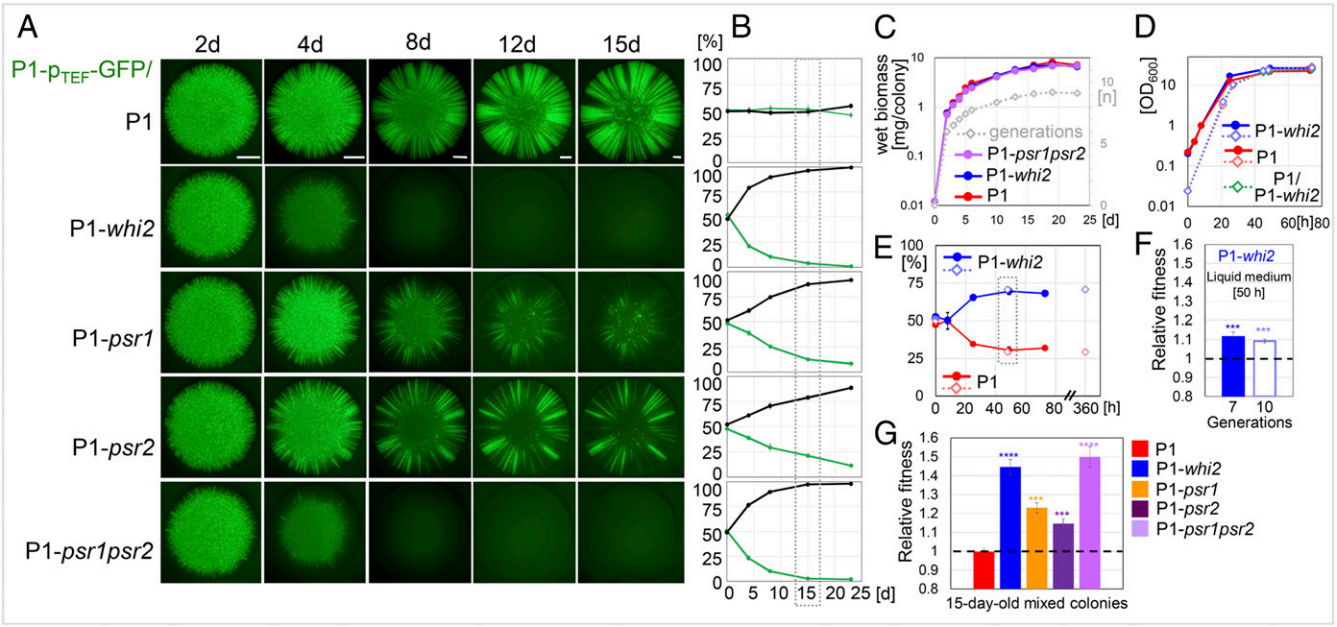

Fig. 3. Competition and fitness of strains defective in WPPC relative to P1. (*A*) Competition in mixed giant colonies of P1-p_{TEF}-GFP (green) and different KO strains (black). P1-p_{TEF}-GFP/P1 mixed colonies are a noncompeting control. (Scale bars, 1 mm.)(*B*) Percentages of P1-p_{TEF}-GFP (green curves) and KO (black curves) cells in mixed colonies featured in *A*. The dotted rectangle indicates the values used for the fitness calculation (in "*G*"). (*C*) Growth of the colonies of P1 and KO strains on GMA. Biomass accrual (left axis), number of generations (right axis). (*D*) Growth of P1 and P1-*whi2* strains in liquid GM. Cultures were inoculated to either OD_{600} (optical density at 600 nm) = 0.2 (solid lines) or OD_{600} = 0.02 (dotted lines). (*E*) Percentages of P1 and P1-*whi2*-p_{TEF}-GFP cells in mixed cultures in liquid GM inoculated to either OD_{600} = 0.2 (filled symbols and solid line) or OD_{600} = 0.02 (open symbols). The dotted rectangle indicates the values used for the fitness calculation (in "*F*"). (*F*) Average fitness of P1-*whi2* relative to P1 in liquid GM at 50 h after seven generations (inoculation OD_{600} = 0.2) or after 10 generations (inoculation OD_{600} = 0.02). Average of three independent experiments shown. SD: ***$P \leq 0.001$. (*G*) Average fitness of KO strains relative to P1-p_{TEF}-GFP in colonies. The fitness of P1 relative to P1-p_{TEF}-GFP is a control. Averages of three independent experiments shown. SD: ***$P \leq 0.001$; ****$P \leq 0.0001$.

As in the colonies, no growth difference was detected for P1 and P1-*whi2* cells in single-strain liquid GM cultures (Fig. 3*D*). P1-*whi2* outcompeted P1 in mixed cultures (Fig. 3*E*), but the fitness differential (Fig. 3*F*) was lower than that in colonies (Fig. 3*G*). Mixed cultures (1:1) inoculated at initial cell densities of OD_{600} ~0.2 and ~0.02 took 7 and 10 generations, respectively, to reach approximately the same OD_{600} after 50 h (Fig. 3*D*). Although differing in the number of generations, the competition advantage of P1-*whi2* over P1 was similar in both liquid cultures and remained almost unchanged over an additional 15 d of cultivation (Fig. 3*E*). The relative fitness of P1-*whi2* reached ~1.1 (Fig. 3*F*).

P1-Derived Papillae Cells Competitively Exclude P1 but Are Outcompeted by P1-*whi2* and P1-*psr1psr2*. Next, we asked whether P1-*whi2* or P1-derived PCs had a greater competitive advantage in mixed colonies. We mixed papillae clones at a 1:1 ratio with P1-p_{TEF}-GFP (Fig. 4*A* and *SI Appendix*, Fig. S6) or with P1-*whi2*-p_{TEF}-GFP (Fig. 4*C* and *SI Appendix*, Fig. S6) and grew chimeric colonies on GMA. All papillae clones exhibited competitive advantages over P1-p_{TEF}-GFP, strongly suggesting that these clones had acquired heritable genetic and/or epigenetic alterations, beneficial in colonies. However, the P1-*whi2*-p_{TEF}-GFP strain exhibited competitive superiority in all chimeric colonies, outcompeting not only P1, but also all papillae clones and excluding competing strains much more rapidly than the papillae clones excluded P1-p_{TEF}-GFP.

Because papillae arose mainly in the U cells of P1 colonies (Fig. 2*C*), we investigated the spatiotemporal dynamics of interstrain competition through vertical cross sectioning of chimeric colonies and fluorescence microscopy (Fig. 4 *B* and *E*). PCs began to exclude P1 cells in the upper areas of 14-d-old colonies (Fig. 4*B*-cont.), correlating with colony differentiation to U and L cells; further competitive exclusion was confined mainly to the U cell subpopulation. In contrast, the exclusion of both P1 cells and PCs by P1-*whi2*-p_{TEF}-GFP cells from the upper regions was already apparent in 4-d-old colonies and continued as colony development progressed (Fig. 4*D*). Papillae clones were significantly fitter in 15-d-old colonies than was strain P1 ($P < 0.0001$; Fig. 4*F*), but the average relative fitness of PCs was markedly lower than that of P1-*whi2* or P1-*psr1psr2* cells (Fig. 4*F* vs. Fig. 3*G*).

The *whi2* and *psr1psr2* Competitive Advantage Is Not Limited to Chimeric Colonies. We then examined whether the substantial P1-*whi2* and P1-*psr1psr2* competitive advantage, relative to all Whi2p-expressing strains, required direct contact among cells in mixed colonies. We grew P1, P1-*whi2*, and P1-*psr1psr2* giant colonies in different combinations and at different distances from one another and monitored changes in colony size over time (Fig. 4*G*). Growing several colonies of a single strain on the same plate had no significant effect on the colony expansion rate (regardless of the experimental setup and distance between colonies), and all strains exhibited similar rates of expansion. However, growing either P1-*whi2* or P1-*psr1psr2* colonies in close proximity to P1 colonies diminished the expansion rate of P1 colonies since approximately the sixth day of colony growth. Later, P1 colony growth was almost completely blocked by the presence of P1-*whi2* (P1-*psr1psr2*) colonies.

A Diffusible Compound May Inhibit P1 Cells in Chimeric Colonies. We then determined whether antagonistic interactions between P1 and P1-*whi2* might be mediated by extracellular diffusible

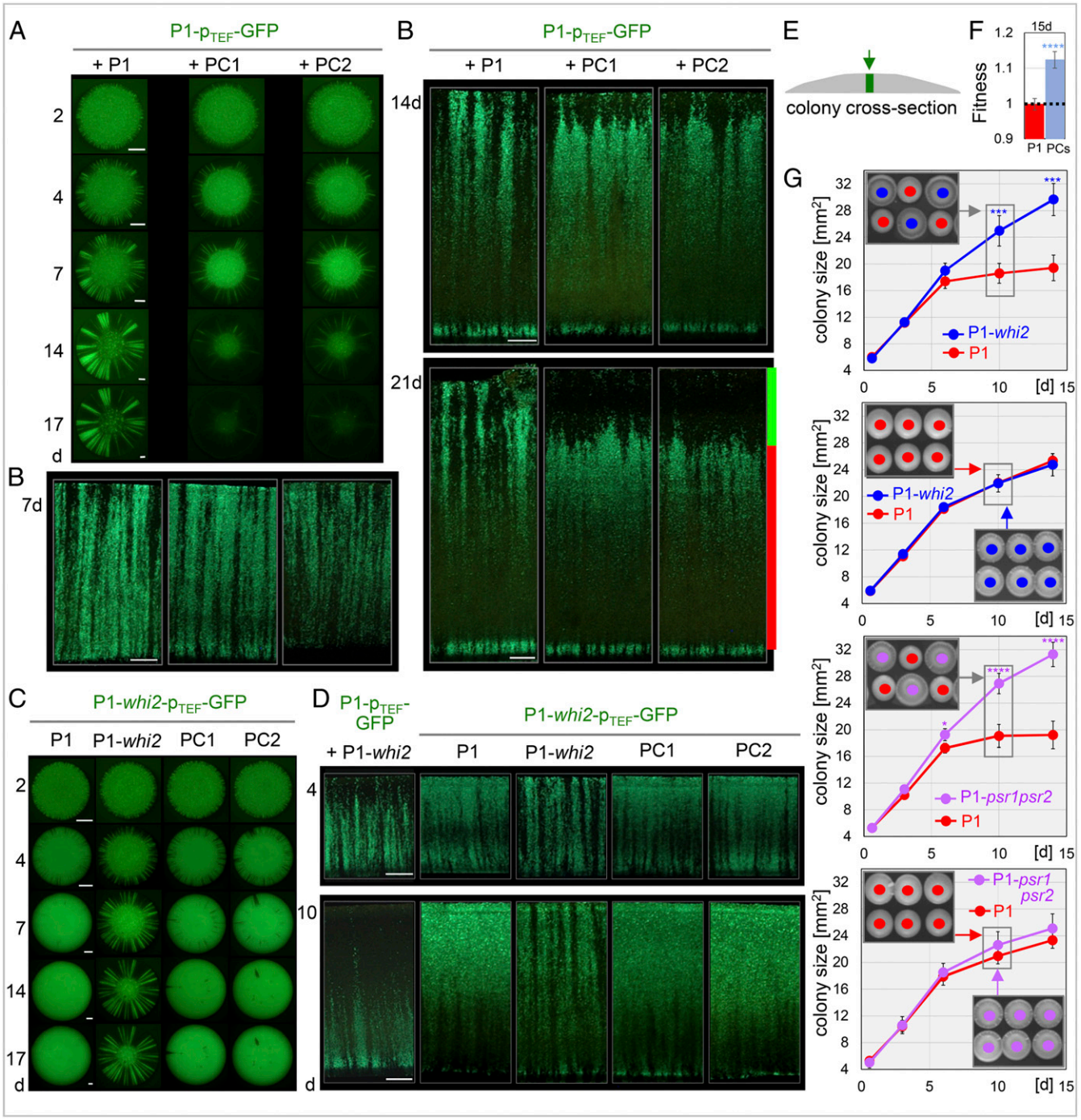

Fig. 4. Spatiotemporal dynamics of the competition of P1, PC clones, and strains defective in WPPC. (*A*) Competition in mixed giant colonies of P1-p_{TEF}-GFP (green) and two independent PC clones (black). Colony competition with other independent PC clones is shown in *SI Appendix*, Fig. S6. Bar, 1 mm. (*B*) Vertical cross sections of central parts (as in scheme *E*) of mixed colonies as in *A* showing the area in which competition occurs. U cells are indicated with green bars, and L cells are indicated with red bars. P1-p_{TEF}-GFP/P1 mixed colonies are a noncompeting control. (Scale bar, 1 mm.) (*C*) Competition in mixed giant colonies of P1-*whi2*-p_{TEF}-GFP (green) and PC clones (black) or P1 strain. P1-*whi2*-p_{TEF}-GFP/P1-*whi2* mixed colonies are noncompeting controls. (Scale bars, 1 mm.) (*D*) Cross sections of central parts (as in scheme *E*) of mixed colonies as in *C* showing the area in which competition occurs. P1-*whi2*-p_{TEF}-GFP/P1-*whi2* mixed colonies are noncompeting controls. Cross sections of P1-p_{TEF}-GFP/P1-*whi2* mixed colonies (as in Fig. 3*A*) are an additional control, showing that the competition profile is independent of which strain is labeled by GFP. (Scale bar, 100 μm.) (*E*) Schematic of a vertical colony cross section indicating (in green) the position of areas shown in *B* and *D*. (*F*) Average fitness of 10 independent PC clones relative to P1-p_{TEF}-GFP (blue) in 15-d-old colonies. Fitness of P1 relative to P1-p_{TEF}-GFP (red) is the control. SD: $^{****}P \leq 0.0001$. (*G*) Mutual effect on colony expansion among P1, P1-*whi2*, and P1-*psr1psr2* colonies grown in close proximity on GMA. Graphs show the growth of colonies, positioned as indicated in the *Inset* images. The coloring of the colonies corresponds to their respective curves. Rectangles indicate the age of the colonies in the images (10 d). Curves were calculated from a representative experiment as the averages of, at least, seven colonies. SD: $^{*}P \leq 0.05$; $^{***}P \leq 0.001$; $^{****}P \leq 0.0001$.

compound(s). First, we prepared a cell-free wash from 3-d-old P1 and P1-*whi2* colonies and assessed the competition between P1-p_{TEF}-GFP and P1-*whi2* in chimeric colonies in the presence of these washes. As shown in the cross sections, treatment with the P1-*whi2* wash (compared to the P1 wash) reduced P1 frequency in 3-d-old chimeric colonies, most notably in upper cell layers (*SI Appendix*, Fig. S7). This result indicates the cumulative effects of the presence of P1-*whi2* cells (also visible in P1-wash-treated chimeric colonies) and of the P1-*whi2* wash (*SI Appendix*, Fig. S7*C*). Next, we grew P1 and P1-*whi2* colonies for 3 d on filters. After colony removal, fresh P1 or P1-*whi2* cells were inoculated on colony footprints, and the number of divisions of individual cells after 6 h was determined. P1 cell division on P1-*whi2* footprints was reduced by ∼20% compared with that on P1 footprints, whereas the accrual of P1-*whi2* cells was the same in both cases (Fig. 5*A*).

To investigate whether liquid culture competition is density dependent, we repeated the P1-vs.-P1-*whi2* competition as in Fig. 3*D* starting from OD_{600} ∼0.02. After nine generations (49 h), we supplemented the culture with fresh GM (to adjust the level of nutrients to that at the beginning of the experiment) and measured cell frequencies over the following 67 h. The frequency of P1-*whi2* reached ∼80% in this experimental setup (Fig. 5*B*) compared with ∼70% in standard cultivation (Fig. 3*E*). The increase in P1 cell number was only ∼2.7% of the increase in P1-*whi2* cell number during the later (high-density) phase, compared with ∼54% in the initial (low-density) phase (Fig. 5*C*). The relative fitness of P1-*whi2* compared with that of P1 was ∼1.1 during the initial interval (Fig. 3*F*) and ∼2 in dense culture.

To assess processes regulated by WPPC, we then compared P1, P1-*whi2*, and P1-*psr1psr2* colonies (4-d-old on GMA) using proteomics. The abundance of 37 proteins increased >5× in both P1-*whi2* and P1-*psr1psr2* relative to P1. These proteins were enriched ($P < 0.01$) for the gene ontology (GO) function term "(transmembrane) transporter activity" and GO component terms "plasma membrane" and "cell periphery" (*SI Appendix*, Table S3A). Other proteins up-regulated >1.8× in both P1-*whi2* and P1-*psr1psr2* ($P < 0.01$) were enriched for GO terms related to metabolic/biosynthetic processes involved in the formation of alcohols and organic hydroxy compounds (*SI Appendix*, Table S3B). In P1 colonies, compared with both P1-*whi2* and P1-*psr1psr2* colonies, only 9 proteins increased by >5× and another 22 proteins increased >1.8× ($P < 0.01$). The combined list of these 31 proteins was enriched for the GO component terms "extracellular region" and cell periphery ($P < 0.01$) and GO process term "coenzyme (cofactor) metabolic process" (*SI Appendix*, Table S4).

Discussion

Cell differentiation, interactions, and coordination underlie the development of spatially organized microbial populations. We found that cells that escape the rules and regulations of yeast colony formation sometimes expand and form papillae within the differentiated U cell subpopulation. The WPPC regulates cell interactions in mixed populations and plays a key role in the behavior of these "rogue" cells.

Colony Differentiation Creates Specific Niches with Conditions that Favor the Expansion of PCs. Mutations (and epigenetic changes) in colonies might be an adaptive bet-hedging strategy (6, 13), generating a variety of diverse low-frequency cell types adapted toward unforeseen environmental changes. Papillae may originate from a fraction of these cells that gain a fitness advantage

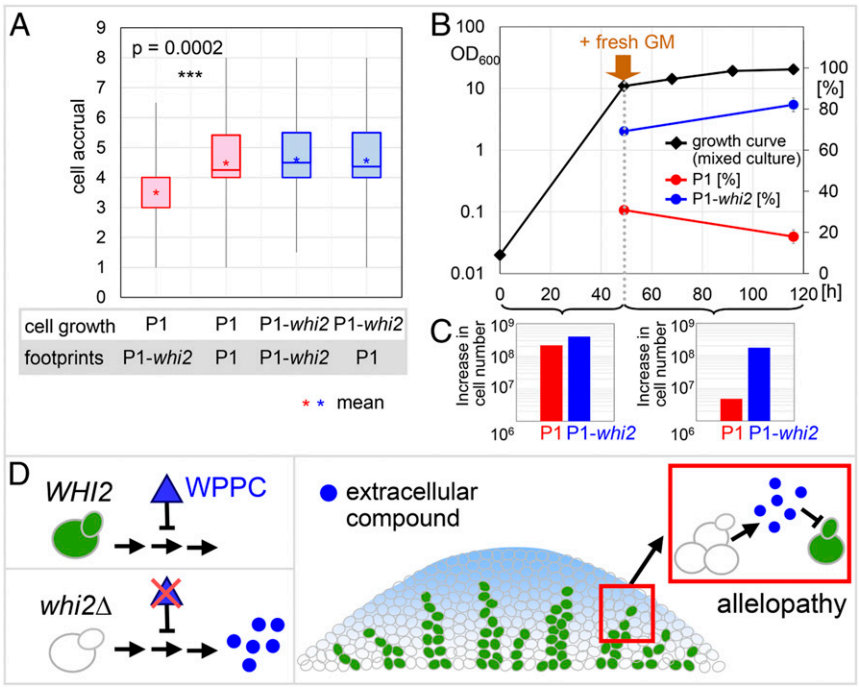

Fig. 5. WPPC in interference competition in chimeric colonies—experimental data and model. (*A*) Average cell divisions of P1 and P1-*whi2* during 6-h cultivation on footprints of P1 or P1-*whi2* colonies (grown on filters). Band within box: median; *, mean. P1 growth on P1-*whi2* footprint was significantly reduced (***$P = 0.0002$); other differences were not significant. Each box plot shows an average of divisions of 80 individual cells. (*B*) Effect of liquid culture density on P1 and P1-*whi2* competition. Mixed culture growth curve (left axis) and percentages of P1 and P1-*whi2* (right axis). Enrichment of the mixed culture with 1/10 volume of 10 × GM medium marked by the brown arrow. (*C*) Accrual of P1 and P1-*whi2* cells over 0–49 h (*Left*) and 49–67 h (*Right*) of growth. (*D*) The WPPC represses (and can, thus, modulate) the production of an extracellular compound (EC) among adjacent cells. Absence of the complex leads to overproduction of the EC and provides cells within chimeric colonies with a competitive advantage via an interference competition mechanism—allelopathy. EC concentration (in blue) depends on the number of P1-*whi2* producer cells in the respective area of the colony.

specifically in the U cell layer, although their ancestors may originate earlier in the colony interior. The competitive success of PCs can be explained by metabolic reprogramming and interactions between U and L cells with L cells providing nutrients to U cells (21, 23) (Fig. 1*A*). Presumably, PCs utilize these nutrients (public goods) more rapidly and/or less sparingly than other cells and gain a fitness advantage in direct competition with U cells, demonstrated by the uncontrolled expansion of papillae populations. In this respect, PCs resemble cheaters, but whether and how they contribute to the production of extracellular nutrients (public goods) remains unclear.

Expansion of papillae results in an increase in size of genetically/epigenetically altered populations, providing a numerical advantage that could, under certain conditions, drive subsequent competitive success. Thus, the presence of numerous papillae could increase a colony's adaptive potential in the face of unpredictable environmental fluctuations (Fig. 1*B*). Further studies are needed to uncover the specific changes that led to the formation of individual papillae clones and to determine whether they are beneficial only within the colony structure or also in diverse conditions faced by cells dispersing from colonies and settling in new territories.

Function of WPPC Independent of Known Downstream Targets. Whi2p has been credited with pleiotropic functions, targeting, together with Psr1p/Psr2p, the transcription factor Msn2p/Msn4p (30) and negatively regulating TORC1 in yeast and other fungi (35, 36, 39). We have shown here that the success of PCs in colonies depends on a functional WPPC but not on Msn2p and/or Msn4p. TORC1 activity in colonies (19) is also unaffected by WPPC functionality, and thus, the competitive superiority of P1-*whi2* or P1-*psr1psr2* cells is independent of TORC1.

Why Does Functional WPPC Support Papillae Formation? We considered two mechanisms that might explain the higher frequency of papillae in papillating colonies than in smooth colonies: an increased mutation rate in Whi2p-expressing strains or an enhanced expansion of cells with mutations/epigenetic changes among Whi2p-expressing U cells. Mutation rates in U and L cells of P1 and P1-*whi2* colonies and the numbers of mutations present among P and S clones were comparable, making a Whi2p role in mutagenesis improbable. However, the finding that strains with nonfunctional WPPC competitively excluded P1 and P1-derived papillae clones strongly supported the second mechanism. P1 and P1-*whi2* (P1-*psr1psr2*) strains exhibited comparable growth rates and development in single-strain colonies and liquid cultures. The competitive superiority of strains with a nonfunctional WPPC and fitness inequalities between the P1 and the P1-*whi2* (P1-*psr1psr2*) genotypes were, thus, not caused by differences in growth rate but were specifically dependent on strain interactions in mixed populations. Similar interaction-specific fitness inequality, caused by social exploitation during social interactions, occurs in genetically diverse mixed bacterial populations and is sometimes referred to as cheating (8). The competitive exclusion of all P1 strains (parental and papillae) by P1-*whi2* in chimeric colonies occurs much earlier (by day 3 or 4) than the exclusion of P1 by papillae clones (by day 12–14). This explains the rare presence of papillae in P1-*whi2* (P1-*psr1psr2*) colonies—cells would need to acquire additional properties to enable them to outcompete a P1-*whi2* (P1-*psr1psr2*) genotype, which is a highly successful interaction competition winner.

Interaction-specific fitness inequality is markedly more pronounced in mixed colonies than in mixed liquid cultures with the same nutritive composition. Relative (to P1) fitness values of P1-*whi2* and P1-*psr1psr2* cells in mixed colonies reached a maximal value of ∼1.5, compared to ∼1.1 for P1-*whi2* in mixed liquid cultures. An increase in the number of generations (before reaching a maximal OD_{600}) in liquid culture or the extension of cultivation for up to 15 d had little effect on the relative fitness of P1-*whi2*. The relative fitness of P1-*whi2* in GM liquid culture approximately corresponds to that of the *whi2*Δ strain in three different liquid media as measured in a barcoded library screen (40).

A Diffusible Extracellular Compound May Mediate the Competitive Superiority of P1-*whi2* Cells in Dense Populations. Single-strain colonies of P1-*whi2* (P1-*psr1psr2*) have a competitive advantage over P1 colonies located in close proximity. In addition, competition in mixed liquid cultures strongly depended on cell density, as demonstrated by comparing competition in low- and high-density cultures. Medium replenishment of high-density mixed liquid culture led to a fitness inequality between P1 and P1-*whi2* that was comparable to (or even greater than) that found in colonies. We, therefore, considered the increased production of a compound that inhibits P1 cells as a possible mechanism through which P1-*whi2* exhibited competitive superiority over P1 (Fig. 5*D*).

Two other results support this hypothesis: 1) Cultivation on P1-*whi2* postcultivation footprints reduced the growth of P1 cells but not that of P1-*whi2*, and 2) treatment with cell-free wash from P1-*whi2* colonies increased the competitive advantage of P1-*whi2* in chimeric colonies compared with treatment with wash from P1 colonies. A proteomic comparison of the colonies further supports the hypothesis. Differentially expressed proteins in P1-*whi2* and P1-*psr1psr2* vs. P1 were enriched for GO terms related to cell surface/membrane properties and metabolism. In particular, a group of plasma membrane transporters, including multidrug resistance transporters potentially expelling metabolites from cells, was highly up-regulated (or detected only) in P1-*whi2* and P1-*psr1psr2* colonies vs. P1 colonies.

How Does the WPPC Function? We hypothesize (Fig. 5*D*) that WPPC negatively regulates the production of an extracellular metabolite that inhibits (via an unknown mechanism) the growth of adjacent cells/colonies. This hypothesis is also supported by a recent prediction that WPPC senses an (as yet unidentified) environmental signal that affects intracellular events during infection-related morphogenesis in the fungus *Colletotrichum orbiculare* (39). According to our model, the synchronized development of cells in a particular area is unaffected when all resident cells exhibit similar sensitivity to and produce similar levels of the metabolite. However, when a less sensitive relatively higher producer (P1-*whi2* or P1-*psr1psr2*) occurs in close proximity to a more sensitive relatively low producer (P1 or P1-derived papillae clones), the growth of the latter is retarded. Consequently, cells with premature stop codons or frameshifts in the *WHI2* gene tend to dominate the population due to their inhibition of other cells. This interference competition model also explains the frequent appearance of *WHI2* secondary mutations in strains of the yeast deletion collection (25, 27–29, 41) and the fixation of *whi2* after its appearance in liquid culture in laboratory evolutionary experiments (26). The effect of such a mechanism is more pronounced in dense structured colonies in which extracellular metabolite gradients form more readily and local concentrations are markedly higher than in standard shaken liquid cultures. Hence, cells defective in WPPC heavily outcompete any Whi2p-expressing cells in chimeric colonies, including cells with beneficial mutations that might otherwise expand to form papillae in U cells (or in other altered conditions). As a result, these cells disappear from mixed populations, reducing genetic cell heterogeneity and the adaptive potential of the population as a whole. Competitive dominance of WPPC-defective cells is, therefore, disadvantageous from a long-term perspective. However, this dominance could be offset under specific circumstances because WPPC-defective cells are more sensitive to stresses, particularly oxidative stress (42).

To summarize, structured yeast colonies can serve as a powerful system for studying spatial pattern formation, cell competition/cooperation, the evolution of beneficial genetic/epigenetic changes, and the regulatory mechanisms underlying these processes. The WPPC is an important regulator with the capability of balancing cell competition/cooperation and modulating expansion of PCs with beneficial traits. It could, thus, be hypothesized that WPPC activity is regulated during population development and could contribute to pattern formation and cell synchronization within a particular niche.

Material and Methods

Yeast Strains, Constructions, and Cultivations. All *S. cerevisiae* strains are listed in *SI Appendix*, Table S1. Clones P1–P3 and S1–S3 were selected after plating the BY4742 strain on GMA plates. Strains with gene deletions, p_{TEF}-GFP, and p_{TEF}-controlled *WHI2*/GFP fusions were derived from strains P1 and S1 as described in the *SI Appendix*.

Giant yeast colonies were inoculated as drops (10 or 1 μL) of cell suspension, six per plate, and grown at 28 °C on GMA (1% yeast extract, 3% glycerol, 1% ethanol, 2% agar, and 10 mM $CaCl_2$) directly or on filters. Papillae clones were separated from P1 colonies by micromanipulation. Microcolonies were plated at densities of 10^2–10^3 cells per GMA plate. Shaken liquid cultures were grown in GM medium (GMA without agar) at 28 °C. For density assessment experiments, the cultures were enriched by addition of 1/10 of 10 × GM medium. Details described in the *SI Appendix*.

Cell Competition Experiments and Relative Fitness Estimation. Mixed giant colonies were inoculated on GMA as drops of cell suspension containing equal numbers of cells of two particular strains. Mixed liquid cultures were inoculated by two strains (mixed 1:1) in GM medium. Competition was determined as described in the *SI Appendix*. Strain fitness, relative to the wild type (WT), was calculated according to ref. 40 as $w = (P'P_{wt}/PP'_{wt})^{1/t}$, where P, P', P_{wt}, and P'_{wt} are initial and final frequencies of the strain, the initial, and the final frequencies of the WT, respectively, and t is the number of generations in the competition. WT represents strain P1-p_{TEF}-GFP (Figs. 3 *F* and *G* and 4*F*). Relative fitness was calculated at 15 d into colony population development.

Imaging of Colonies and Colony Vertical Cross Sections. Imaging of colonies and colony cross sections prepared as described in ref. 21 using a ProgRes CT3 CMOS camera, Leica stereo microscope, and Zeiss Axio Observer.Z1 microscope. Details described in the *SI Appendix*.

Whole-Genome Resequencing of S and P Clones. DNA was extracted from biomass of clones grown in yeast extract–peptone–dextrose (YPD) medium and sequenced using an Illumina as described in the *SI Appendix*.

Proteomics. Proteins of cells harvested from colonies were analyzed by nanoliquid chromatography coupled to tandem mass spectrometry (LC-MS/MS) using an Orbitrap Fusion Tribrid mass spectrometer (Thermo Scientific) as described in the *SI Appendix*.

Data Availability. The sequencing data were deposited in the National Center for Biotechnology Information's Sequence Read Archive, https://www.ncbi.nlm.nih.gov/bioproject/PRJNA542361 (accession no. PRJNA542361). The proteomics data were deposited at the ProteomeXchange Consortium via the Proteomics Identifications Database, http://www.ebi.ac.uk/pride/archive/projects/PXD016670 (accession no. PXD016670).

ACKNOWLEDGMENTS. We thank Alexandra Pokorná for excellent technical support. NG sequencing was performed in Norwegian Sequencing Centre, Oslo. LC-MS/MS was performed at the BIOCEV Proteomics Facility. This study was supported by LTAUSA18162 and by LQ1604 NPU II provided by MEYS and by RVO 61388971; research was performed in BIOCEV supported by CZ.1.05/1.1.00/02.0109 provided by ERDF and MEYS.

1. T. S. Tshikantwa, M. W. Ullah, F. He, G. Yang, Current trends and potential applications of microbial interactions for human welfare. *Front. Microbiol.* **9**, 1156 (2018).
2. S. Elias, E. Banin, Multi-species biofilms: Living with friendly neighbors. *FEMS Microbiol. Rev.* **36**, 990–1004 (2012).
3. S. Höfs, S. Mogavero, B. Hube, Interaction of *Candida albicans* with host cells: Virulence factors, host defense, escape strategies, and the microbiota. *J. Microbiol.* **54**, 149–169 (2016).
4. L. K. Ursell, J. L. Metcalf, L. W. Parfrey, R. Knight, Defining the human microbiome. *Nutr. Rev.* **70** (suppl. 1), S38–S44 (2012).
5. S. Zhang, N. Merino, A. Okamoto, P. Gedalanga, Interkingdom microbial consortia mechanisms to guide biotechnological applications. *Microb. Biotechnol.* **11**, 833–847 (2018).
6. C. E. Tarnita, The ecology and evolution of social behavior in microbes. *J. Exp. Biol.* **220**, 18–24 (2017).
7. R. Popat *et al*., Quorum-sensing and cheating in bacterial biofilms. *Proc. Biol. Sci.* **279**, 4765–4771 (2012).
8. R. R. Nair, F. Fiegna, G. J. Velicer, Indirect evolution of social fitness inequalities and facultative social exploitation. *Proc. Biol. Sci.* **285**, 20180054 (2018).
9. E. A. Ostrowski *et al*., Genomic signatures of cooperation and conflict in the social amoeba. *Curr. Biol.* **25**, 1661–1665 (2015).
10. D. Greig, M. Travisano, Density-dependent effects on allelopathic interactions in yeast. *Evolution* **62**, 521–527 (2008).
11. O. Rendueles, M. Amherd, G. J. Velicer, Positively frequency-dependent interference competition maintains diversity and pervades a natural population of cooperative microbes. *Curr. Biol.* **25**, 1673–1681 (2015).
12. P. Cao, A. Dey, C. N. Vassallo, D. Wall, How myxobacteria cooperate. *J. Mol. Biol.* **427**, 3709–3721 (2015).
13. J. van Gestel, H. Vlamakis, R. Kolter, Division of labor in biofilms: The ecology of cell differentiation. *Microbiol. Spectr.* **3**, MB-0002-2014 (2015).
14. W. C. Ratcliff, R. F. Denison, M. Borrello, M. Travisano, Experimental evolution of multicellularity. *Proc. Natl. Acad. Sci. U.S.A.* **109**, 1595–1600 (2012).
15. W. C. Ratcliff, J. D. Fankhauser, D. W. Rogers, D. Greig, M. Travisano, Origins of multicellular evolvability in snowflake yeast. *Nat. Commun.* **6**, 6102 (2015).
16. J. H. Koschwanez, K. R. Foster, A. W. Murray, Sucrose utilization in budding yeast as a model for the origin of undifferentiated multicellularity. *PLoS Biol.* **9**, e1001122 (2011). Correction in: *PLoS Biol.* **9** (2011).
17. L. Váchová, Z. Palková, How structured yeast multicellular communities live, age and die? *FEMS Yeast Res.* **18**, foy033 (2018).
18. Z. Palková *et al*., Ammonia mediates communication between yeast colonies. *Nature* **390**, 532–536 (1997).
19. L. Váchová, L. Hatáková, M. Cáp, M. Pokorná, Z. Palková, Rapidly developing yeast microcolonies differentiate in a similar way to aging giant colonies. *Oxid. Med. Cell. Longev.* **2013**, 102485 (2013).
20. Z. Palková, L. Váchová, Yeast cell differentiation: Lessons from pathogenic and non-pathogenic yeasts. *Semin. Cell Dev. Biol.* **57**, 110–119 (2016).
21. M. Cáp, L. Stěpánek, K. Harant, L. Váchová, Z. Palková, Cell differentiation within a yeast colony: Metabolic and regulatory parallels with a tumor-affected organism. *Mol. Cell* **46**, 436–448 (2012).
22. M. Cáp, L. Váchová, Z. Palková, Yeast colony survival depends on metabolic adaptation and cell differentiation rather than on stress defense. *J. Biol. Chem.* **284**, 32572–32581 (2009).
23. M. Čáp, L. Váchová, Z. Palková, Longevity of U cells of differentiated yeast colonies grown on respiratory medium depends on active glycolysis. *Cell Cycle* **14**, 3488–3497 (2015).
24. H. Yang *et al*., Papillation in *Bacillus anthracis* colonies: A tool for finding new mutators. *Mol. Microbiol.* **79**, 1276–1293 (2011).
25. S. A. Comyn, S. Flibotte, T. Mayor, Recurrent background mutations in *WHI2* impair proteostasis and degradation of misfolded cytosolic proteins in *Saccharomyces cerevisiae*. *Sci. Rep.* **7**, 4183 (2017).
26. G. I. Lang *et al*., Pervasive genetic hitchhiking and clonal interference in forty evolving yeast populations. *Nature* **500**, 571–574 (2013).
27. B. Szamecz *et al*., The genomic landscape of compensatory evolution. *PLoS Biol.* **12**, e1001935 (2014).
28. X. Teng *et al*., Genome-wide consequences of deleting any single gene. *Mol. Cell* **52**, 485–494 (2013).
29. J. van Leeuwen *et al*., Exploring genetic suppression interactions on a global scale. *Science* **354**, aag0839 (2016).
30. D. Kaida, H. Yashiroda, A. Toh-e, Y. Kikuchi, Yeast Whi2 and Psr1-phosphatase form a complex and regulate STRE-mediated gene expression. *Genes Cells* **7**, 543–552 (2002).
31. N. Mendl *et al*., Mitophagy in yeast is independent of mitochondrial fission and requires the stress response gene *WHI2*. *J. Cell Sci.* **124**, 1339–1350 (2011).
32. Y. Chen, L. Stabryla, N. Wei, Improved acetic acid resistance in *Saccharomyces cerevisiae* by overexpression of the *WHI2* gene identified through inverse metabolic engineering. *Appl. Environ. Microbiol.* **82**, 2156–2166 (2016).
33. P. Lis *et al*., Screening the yeast genome for energetic metabolism pathways involved in a phenotypic response to the anti-cancer agent 3-bromopyruvate. *Oncotarget* **7**, 10153–10173 (2016).

34. P. Radcliffe, J. Trevethick, M. Tyers, P. Sudbery, Deregulation of *CLN1* and *CLN2* in the *Saccharomyces cerevisiae whi2* mutant. *Yeast* **13**, 707–715 (1997).
35. X. Chen *et al*., Whi2 is a conserved negative regulator of TORC1 in response to low amino acids. *PLoS Genet.* **14**, e1007592 (2018).
36. X. Teng, J. M. Hardwick, Whi2: A new player in amino acid sensing. *Curr. Genet.* **65**, 701–709 (2019).
37. Z. Liu, Y. Xiang, G. Sun, The KCTD family of proteins: Structure, function, disease relevance. *Cell Biosci.* **3**, 45 (2013).
38. G. I. Lang, A. W. Murray, Estimating the per-base-pair mutation rate in the yeast *Saccharomyces cerevisiae*. *Genetics* **178**, 67–82 (2008).
39. K. Harata, T. Nishiuchi, Y. Kubo, *Colletotrichum orbiculare WHI2*, a yeast stress-response regulator homolog, controls the biotrophic stage of hemibiotrophic infection through TOR Signaling. *Mol. Plant Microbe Interact.* **29**, 468–483 (2016).
40. W. Qian, D. Ma, C. Xiao, Z. Wang, J. Zhang, The genomic landscape and evolutionary resolution of antagonistic pleiotropy in yeast. *Cell Rep.* **2**, 1399–1410 (2012).
41. W. C. Cheng *et al*., Fis1 deficiency selects for compensatory mutations responsible for cell death and growth control defects. *Cell Death Differ.* **15**, 1838–1846 (2008).
42. C. L. Tucker, S. Fields, Quantitative genome-wide analysis of yeast deletion strain sensitivities to oxidative and chemical stress. *Comp. Funct. Genomics* **5**, 216–224 (2004).